INSIGHTS ON METAL DOPED GRAPHENE IN THE ADSORPTION OF ARSENIC VIA DFT CALCULATION

Ibraheem Olusola Ayeni [ID][a,b] and Toyese Oyegoke [ID][a,b,*]

[a]CAD-Engineering of Processes and Reactive Materials Group, Chemical Engineering Department, Ahmadu Bello University, Samaru Campus, Sabon-gari, 810106, Zaria, Kaduna State, Nigeria
[b]Green Science Forum-Modeling and Simulation, Pencil Team, Ahmadu Bello University, Samaru Campus, Sabon-gari LGA, 810106, Zaria, Kaduna State, Nigeria
[*]e-mail: oyegoketoyese@gmail.com; phone: +2348098679625

Accepted version posted online: 09 April 2025

Disclaimer: This is an uncorrected proof version of the manuscript that has been accepted for publication. Chemistry Journal of Moldova provides this version as a service to authors and researchers. Copyediting, typesetting, and the review of the resulting proof will be undertaken on this manuscript before the final publication. During production and pre-press, errors may be found which could affect the content, and all legal disclaimers that apply to the journal relate to this version also.

INSIGHTS ON METAL DOPED GRAPHENE IN THE ADSORPTION OF ARSENIC *VIA* DFT CALCULATION

Ibraheem Olusola Ayeni [a,b] and Toyese Oyegoke [a,b,*]

aCAD-Engineering of Processes and Reactive Materials Group, Chemical Engineering Department, Ahmadu Bello University, Samaru Campus, Sabon-gari, 810106, Zaria, Kaduna State, Nigeria
bGreen Science Forum-Modeling and Simulation, Pencil Team, Ahmadu Bello University, Samaru Campus, Sabon-gari LGA, 810106, Zaria, Kaduna State, Nigeria
*e-mail: oyegoketoyese@gmail.com; phone: +2348098679625

Abstract. Arsenic contamination in drinking water poses significant health risks worldwide, making the development of efficient removal technologies a critical area of research. This study explores the enhancement of graphene's arsenic (As) adsorption capabilities through metal doping at various positions on its surface. Using density functional theory (DFT), the interactions between arsenic and graphene doped with selected metals were simulated, evaluating the influence of different doping positions on adsorption efficiency. The results demonstrated that metal doping significantly improves the arsenic removal capacity of graphene, with variations observed depending on the doping configuration. These findings contribute to a deeper understanding of the adsorption mechanisms in graphene-based materials and offer a computational approach for designing advanced adsorbents for environmental remediation.

Introduction

Arsenic is a major environmental pollutant, often released into the environment through natural processes such as weathering, mineral dissolution, and various biochemical activities [1,2]. Additionally, human activities, including mining, industrial effluents, excessive pesticide and herbicide application, and contaminated groundwater, significantly contribute to arsenic contamination [3]. Arsenic is not only a water pollutant but also an air pollutant, with detrimental effects on both air quality and aquatic life. The dissolution of arsenic in water bodies can harm aquatic ecosystems, while exposure to arsenic has been linked to several serious health conditions, including arsenicosis, leuco-melanosis, and cancers [4-7].

In response to the growing concern over arsenic contamination, numerous studies have focused on controlling its release into the environment [8]. One effective control method is adsorption, which has been applied not only to arsenic removal but also for other pollutants such as chromium [9,10], cadmium [11-14], carbon dioxide [15-18], and other gases [19,20]. For example, Goswami, A. *et al.* demonstrated that copper(II) oxide nanoparticles are highly efficient in removing arsenic from water, achieving an adsorption capacity of 1086.2 μg/g [21]. This process follows a pseudo-second-order kinetic model and conforms to the Langmuir isotherm. Similarly, Altundoğan, H.S. *et al.* showed that activated red mud could effectively remove arsenic in the dosage range of 20 to 100 g/L, with removal efficiencies between 87% and 97%, following first-order kinetics and the Langmuir isotherm [22]. Other adsorbents explored for arsenic removal include synthetic zeolites (Chutia, P. *et al.* [23], 76-80% removal) and magnetic adsorbents made from iron oxide and wheat straw [24], where higher iron content correlated with increased adsorption capacity.

While much of the existing research focuses on experimental methods, computational approaches to arsenic removal remain under-explored. Notable computational studies include Zhang, Y. *et al.* research that deployed the use of density functional theory (DFT) to assess the arsenic removal potential of iron oxide surfaces [25]. Similarly, Watt, H.D. *et al.* [26] computationally examined various mineral surfaces, including alumina [27], phosphorene [28], and carbon-based surfaces [29], for their arsenic adsorption capabilities. Wu, D. *et al.* [29]

also used computational methods to study a carbon-based adsorbent and found that the presence of small amounts of sulphur dioxide significantly enhanced arsenic removal. Despite the advancements in computational studies, there has been limited exploration of molecular-scale mechanisms governing arsenic adsorption. Moreover, while doping graphene surfaces with metals has been shown to alter their electronic properties and improve interactions with pollutants, few studies have investigated how different doping positions on the graphene surface affect these interactions.

This study addressed this gap by establishing a baseline for investigating the sorption strength of arsenic on graphene surfaces doped with selected metals. Using quantum mechanical DFT calculations, the research explores how varying doping positions influence the molecular properties of graphene and its interaction with arsenic. Understanding the complexity of model wastewater as a mixture of multiple components when experimentally characterized, this study simplified the problem by modelling its wastewater (also known as synthetic wastewater) as a two-component system: water and arsenic (that is, the key pollutant), consistent with practices in experimental studies. In this study, we examine the performance of different surface modifications (*i.e.*, the effects of different doping sites) in the quest for improving arsenic removal, shedding light on the potential for optimizing graphene-based adsorbents for environmental clean-up.

Computational methodology and details

This section presents an approach to the investigation of changing the position of the metal on the surface of the modified graphene and its impact on its Arsenic removal ability. These includes the study strategy, energy and geometry optimization method, and adsorption energy analysis.

Study strategy

In this research, the adsorption potential of the pristine graphene and the metal doped graphene were explored. Further investigation of three positions where the metal is bonded to the surface of the graphene sheet were also carried out to ascertain the effects of different positions on the sheet. The structure of these surfaces (pristine and metal doped graphene) after geometry (or structural) optimization is shown in Figure 1. It is important to note that the graphene structures used in this study was modelled as finite-sized

graphene quantum dots with hydrogen-passivated edges. This choice of structure ensures computational tractability and stability while maintaining the essential electronic and adsorption properties of graphene. The hydrogen passivation eliminates dangling bonds at the edges, allowing us to focus on the effect of metal doping in the central region of the graphene sheet.

In this study, it was investigated three distinct positions for metal dopants (Cu, Al, Mn) on the graphene sheet: the centre position (Gra-Cu, Gra-Al, Gra-Mn), where the metal atom replaces a carbon atom at the centre, maximizing interaction with arsenic and causing significant lattice distortion, due to the difference in atomic size between the metal and the carbon atom [30]; the edge position (Gra-Cu1, Gra-Al1, Gra-Mn1), where the metal atom is bonded to carbon atoms at the periphery, allowing strong interactions with arsenic while minimizing lattice distortion; and the intermediate position (Gra-Cu2, Gra-Al2, Gra-Mn2).

Energy and geometry optimization calculation

Geometry optimization and energy calculations were done using density functional theory calculations utilizing the global hybrid functional (B3LYP) and the 6-31G* polarization basis set with a convergence criterion of 5 a.u. on Spartan's V24 modelling package [31] with the help of Lenovo Officebook Laptop.

Adsorption energy calculation

The adsorption energy (E_{ads}), which represents the energy involved in the adsorption of Arsenic in electron volts (eV), is calculated using the formula in Eq.(1).

$$E_{ads} = E_{ax} - E_a - E_x \qquad (1)$$

where, E_{ads} is the adsorption energy or strength;
   E_a is the energy of the pollutant or adsorbate (arsenic);
   E_x represents the energy of the adsorbent (pristine or metal-doped graphene);
   E_{ax} is the energy of the bonded structure formed by the adsorbate and adsorbent.

This formula measures the energy change that occurs when the adsorbate interacts with the adsorbent surface [13,27,32-35]. A negative value for E_{ads} indicates that the adsorption process is exothermic and spontaneous, promoting the stability of the adsorbed state, while a positive value suggests the opposite [30,36].
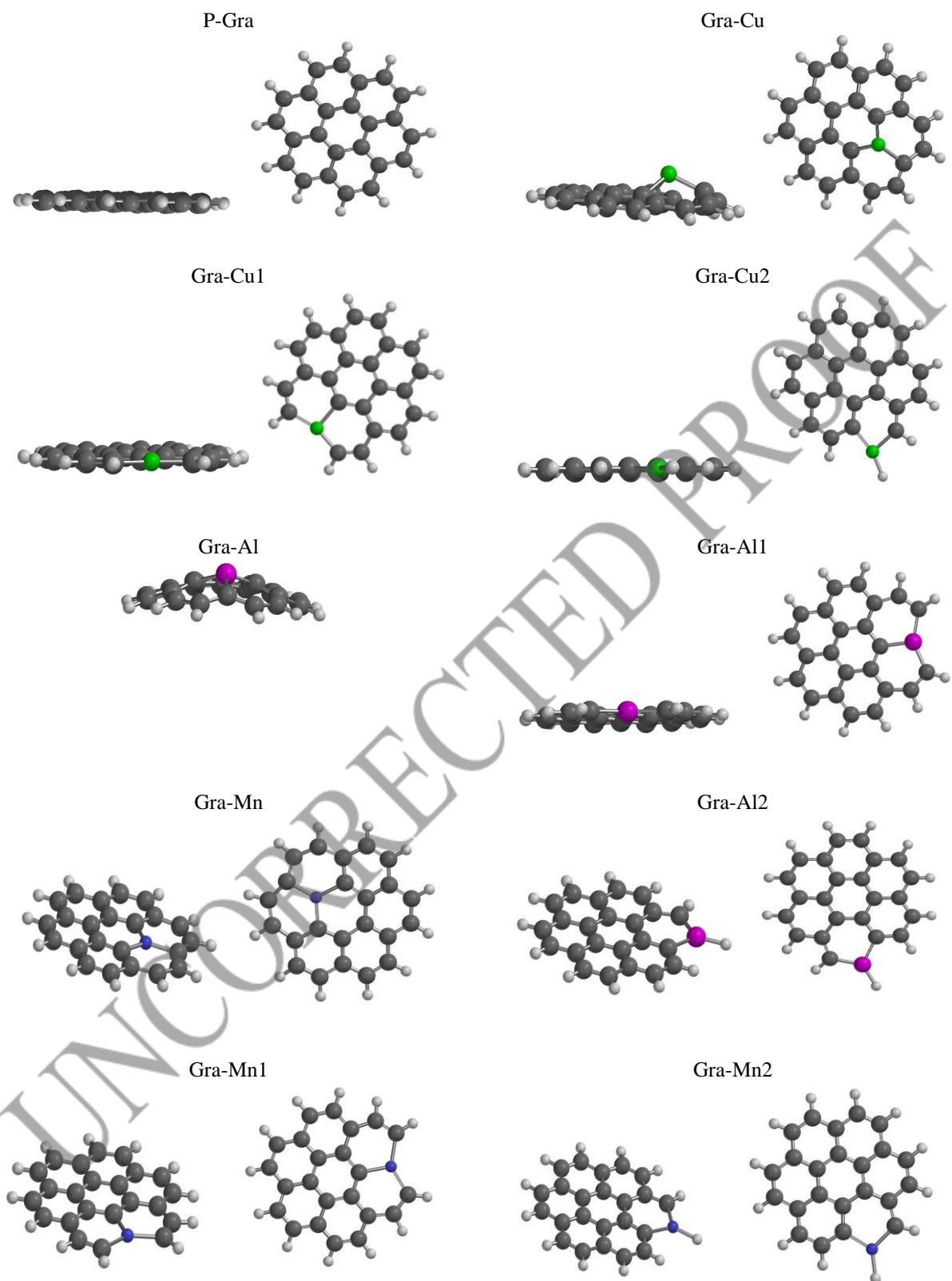
P-Gra

Gra-Cu

Gra-Cu1

Gra-Cu2

Gra-Al

Gra-Al1

Gra-Mn

Gra-Al2

Gra-Mn1

Gra-Mn2

Figure 1. Structure of the interacting surface. Where, P-Gra = Pristine Graphene,
Gra-Cu = Graphene-Copper surface, Gra-Al = Graphene-Aluminium surface,
Gra-Mn = Graphene-Manganese surface (Note that all Copper (Cu), Aluminium (Al), Manganese (Mn),
Carbon (C), and Hydrogen (H) atoms are displaced in green, pink, blue, black, and white).

Results and Discussion
Analysis of the interacting species molecular properties

This section provides information about the structural properties of each surface (adsorbent) presented in Table 2. These properties encompass the ionization potential (IP), electron affinity (EA), highest occupied molecular orbital (HOMO), lowest unoccupied molecular orbital (LUMO), electron negativity (EA), chemical hardness (CH), global electrophilicity index (GEI), energy band gap (Egap) are presented in Table 2 which are computed with the use of the models presented in the literature [37,38] with the aid of Spartan molecular modelling package [31] using its in-built spreadsheet features, ensuring accuracy and minimizing human error and are presented in Table 1.

The analysis of the highest occupied molecular orbital (HOMO) energy (Table 2), which indicates a species' ability to ionize and release electrons to interacting species, reveals that doping the graphene [37-39] surface with metals (Cu, Al, Mn) reduces the negativity of the HOMO energy. Specifically, the surfaces Gra-Cu, Gra-Al1, and Gra-Mn2 exhibit the least negative values at -4.42 eV, -4.66 eV, and -4.82 eV, respectively, compared to the undoped graphene.

Similarly, the analysis of the lowest unoccupied molecular orbital (LUMO) energy, which reflects a species' ability to accept electrons from an interacting species according the literature [37,38], indicates that the metal-doped graphene surfaces exhibit more negative LUMO values. The surfaces Gra-Cu1, Gra-Al, and Gra-Mn2 show the most negative values at -3.11 eV, -1.72 eV, and -3.22 eV, respectively, compared to pristine graphene. This implies that Cu, Al, and Mn-doped surfaces are more likely to accept electrons than donate them. This trend is also consistent with the comparison of Ionization Potential (IP) and Electron Affinity (EA) values (calculated as the negative of the HOMO and LUMO energies, respectively), where Gra-Cu1, Gra-Al, and Gra-Mn2 show the highest electron affinities (1.48 eV, 3.18 eV, and 3.22 eV, respectively).

Furthermore, analysis into the energy band gap of the surfaces in Figure 1 clearly reveals that the Cu, Al and Mn doped surfaces are less stable/more reactive when compared to pristine graphene with Gra-Cu1, Gra-Al1 and Gra-Mn2 being the least stable/most reactive of the surfaces. Table 2 also confirms the relationship between the CH of the surfaces and its Egap, the larger the Egap the harder the molecule [38], with the pristine graphene being the hardest materials with a corresponding larger Egap. In a null shell, the analysis of the different properties of the modified graphene surfaces employed in this study attest that doping graphene with metals enhances its reactivity and adsorption capacity.

Table 1

Molecular properties and their mathematical expressions with Spartan-aided calculation code employed.

Molecular properties	Mathematical Expressions	Spartan Spreadsheet Calculation Code
Highest Occupied Molecular Orbital	$EHOMO = E_{HOMO}$	EHOMO (eV) = @HOMO*@hart2ev
Lowest Unoccupied Molecular Orbital	$ELUMO = E_{LUMO}$	ELUMO(eV)= @LUMO*@hart2ev
Ionization Potential	$IP = - E_{HOMO}$	IP (eV) = -@HOMO* @hart2ev
Electron Affinity	$EA = - E_{LUMO}$	EA (eV) = -@LUMO* @hart2ev
Electronegativity	$EN = (IP+EA)/2$	EN (eV) = (-(@LUMO+HOMO)/2)*@hart2ev
Chemical Hardness	$CH = (IP-EA)/2$	CH (eV) = ((@LUMO-@HOMO)/2)*@hart2ev
Electronic Gap	$Egap = IP – EA$	Egap (eV) = (@LUMO-@HOMO) *@hart2ev

Table 2

Structural properties of each surface (adsorbent) including the pristine and metal doped graphene surface.

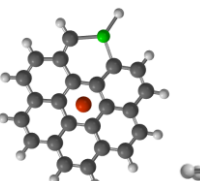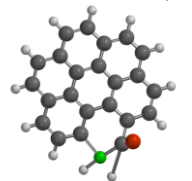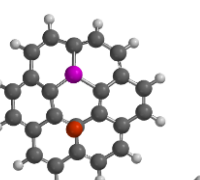| Label	EHOMO (eV)	ELUMO (eV)	IP (eV)	EA (eV)	EN (eV)	CH (eV)	Egap (eV)
P-Gra	-5.4491	-1.4121	5.4491	1.4120	3.4306	2.0185	4.0371
Gra-Cu	-4.4252	-1.9873	4.4252	1.9873	3.2062	1.2189	2.4379
Gra-Cu1	-4.6009	-3.1185	4.6009	3.1185	3.8597	0.7412	1.4824
Gra-Cu2	-4.8920	-2.6424	4.8920	2.6424	3.7672	1.1248	2.2496
Gra-Al	-5.0047	-1.7230	5.0047	1.7230	3.3638	1.6409	3.2817
Gra-Al1	-4.6585	-1.4823	4.6585	1.4823	3.0704	1.5881	3.1763
Gra-Al2	-4.7799	-1.4233	4.7798	1.4233	3.1016	1.6783	3.3565
Gra-Mn	-5.2034	-3.0596	5.2034	3.0596	4.1315	1.0719	2.1438
Gra-Mn1	-5.1506	-3.0361	5.1506	3.0361	4.0934	1.0573	2.1145
Gra-Mn2	-4.8231	-3.2172	4.8231	3.2172	4.0202	0.8030	1.6059

Adsorption studies
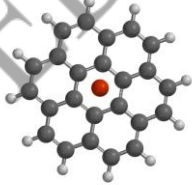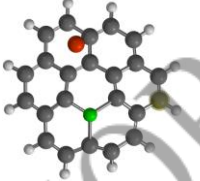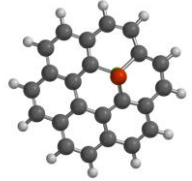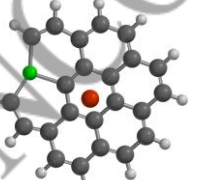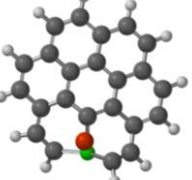
Here, the results obtained from the adsorption study on each surface (absorbent) employed in this research which encompasses the influence of selected metals and its position on the graphene surface are presented. Table 2 shows the geometry of each surface employed in this study before and after adsorption of the pollutant. Note that the distance represented in Table 2 is the closest distance between the absorbent and the pollutant, where As-metal represent the distance between the pollutant and the metal on surface of the absorbent and As-C represents the closest distance between the pollutant and the carbon atom on the surface of the absorbent.

Geometry analysis of the surfaces indicates that as arsenic approaches the metal/carbon atoms on the surface of the adsorbent, the interaction between the surface and the pollutant increases. The bond distance between arsenic and pristine graphene is 4.671 Å, was found to be wider than one obtained by Srivastava & Srivastava [40] as 2.14 Å which could be due to co-adsorption of the arsenic with water on the same surface. However, the metal-doped surfaces show shorter bond distances, indicating stronger interactions with the pollutant. For instance, Gra-Cu has the shortest bond distance of 2.112 Å with arsenic, corroborating existing literature [30]. Gra-Cu1 and Gra-Al exhibit bond distances of approximately 2.5 Å, while Gra-Al1 and Gra-Al2 have a bond distance of around 2.4 Å, and Gra-Cu2 shows a bond distance of 3.42 Å. Among the manganese-doped graphene surfaces, Gra-Mn2 exhibits the shortest bond distance of 2.128 Å.

Table 2

The resulting bond distance and molecular structure of the surface after interaction with the pollutant.

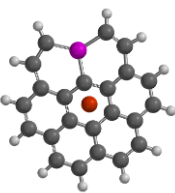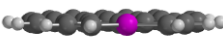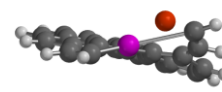| Surface	Before	After
P-Gra	As–C = 3.816 Å	As–C = 4.671 Å
Gra-Cu	As–Cu = 4.481 Å; As – C = 3.675 Å	A –Cu = 2.112 Å; As – C = 3.425 Å
Gra-Cu1	As-Cu = 4.966 Å; As-C = 3.770 Å	As – Cu = 2.491; As – C = 1.920 Å
Gra-Cu2	As-Cu= 5.518 Å; As-C = 3.792 Å	As-Cu= 3.417; As – C = 1.793 Å
Gra-Al	As-Al= 4.066 Å; As-C = 3.611 Å	As-Al= 2.485 Å; As-C = 2.110 Å

Continuation of Table 2
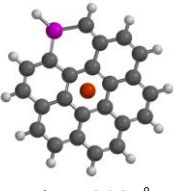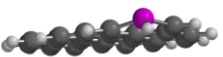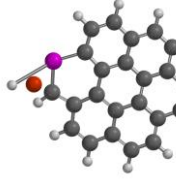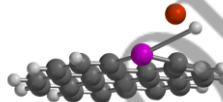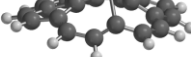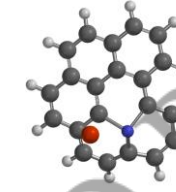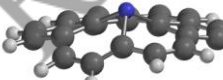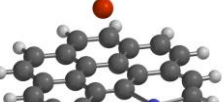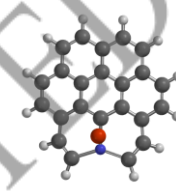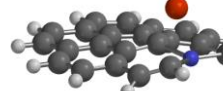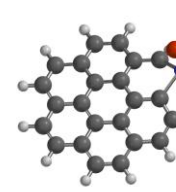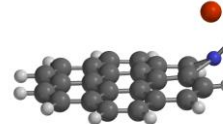
Surface	Before	After
Gra-Al1	As-Al= 4.893 Å; As-C = 3.838 Å	As – Al = 2.367; As – C = 1.861 Å
Gra-Al2	As-Al= 5.208 Å; As-C = 3.815 Å	As -Al = 2.364; As – C = 2.362 Å
Gra-Mn	As-Mn = 4.732 Å; As-C = 3.685 Å	As-Mn = 2.290 Å; As-C = 2.107 Å
Gra-Mn1	As-Mn= 5.050 Å; As-C = 3.862 Å	As-Mn= 2.158 Å; As-C = 2.012 Å
Gra-Mn2	As-Mn= 5.588 Å; As-C = 3.790 Å	As-Mn= 2.128 Å; As-C = 3.160 Å

Table 3

Adsorption strength in eV of each adsorbent.

Label	Eads (eV)	Highest Eads (eV)
P-Gra	-1.04	-1.04
Gra-Cu	-2.85	-4.63 (Gra-Cu1)
Gra-Cu1	-4.63	
Gra-Cu2	-2.23	
Gra-Al	-2.58	-3.10 (Gra-Al2)
Gra-Al1	-2.87	
Gra-Al2	-3.10	
Gra-Mn	-4.69	-4.69 (Gra-Mn)
Gra-Mn1	-3.24	
Gra-Mn2	-4.23	

Table 3 summarizes the adsorption strength (in electron volts) of arsenic on the different surfaces studied. Doping with metals significantly increases the adsorption strength of the surface compared to pristine graphene. The surfaces Gra-Cu1, Gra-Al2, and Gra-Mn exhibit the highest adsorption strengths of -4.63 eV, -3.10 eV, and -4.69 eV, respectively. This trend agrees with the bond distance data (Table 2) and supports the direct relationship between adsorption energy and the bond distance between adsorbate and adsorbent surface, as reported in the literatu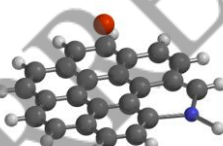re [41,42]. The adsorption strength followed the order: Manganese (Gra-Mn) > Copper (Gra-Cu1) > Aluminium (Gra-Al2) > Not-dopped (P-Gra). In agreement with the literature report [40,43,44], the literatures also showed that doping graphene sheet with metals (such as iron, copper with boron, titanium, and others) improves its adsorptive properties for arsenic removal.

Conclusions

This study provides a comprehensive computational analysis of the influence of metal doping on the arsenic removal capabilities of graphene, with a particular focus on how different doping positions affect the interaction between graphene and arsenic. The study's findings show that doping graphene with metals such as copper (Cu), aluminium (Al), and manganese (Mn) significantly enhances its adsorption strength for arsenic, with the adsorption efficiency varying depending on the doping configuration. Notably, metal-doped graphene surfaces exhibited shorter bond distances and stronger interactions with arsenic compared to pristine graphene, confirming that doping plays a key role in improving the material's adsorption properties.

The computational results, based on density functional theory (DFT) calculations, also reveal that the electronic properties of graphene-such as HOMO/LUMO energy levels and electron affinity-are substantially modified by doping, leading to improved arsenic adsorption. Specifically, the Gra-Cu1, Gra-Al2, and Gra-Mn configurations demonstrated the highest adsorption strengths, making them promising candidates for designing advanced adsorbents for environmental clean-up.

Overall, this research highlights the potential of metal-doped graphene as an efficient adsorbent for arsenic removal from contaminated water, providing new insights into the mechanisms governing the interaction between graphene-based materials and pollutants. The findings also suggest that further optimization of doping positions and metal types could lead to even more efficient materials for a wide range of environmental remediation applications. Future work could explore the practical scalability of these materials and extend the study to other pollutants, further solidifying the role of graphene-based adsorbents in sustainable environmental solutions, including the impact of pH and surface selectivity in the presence of competing mixture components.

References

1. Kanel, S.R.; Das, T.K.; Varma, R.S.; Kurwadkar, S.; Chakraborty, S.; Joshi, T.P.; Bezbaruah, A.N.; Nadagouda, M.N. Arsenic contamination in groundwater: Geochemical basis of treatment technologies. ACS Environmental Au, 2023, 3(3), pp. 135–152. DOI: https://doi.org/10.1021/ACSENVIRONAU.2C00053

2. Zhuang, F.; Huang, J.; Li, H.; Peng, X.; Xia, L.; Zhou, L.; Zhang, T.; Liu, Z.; He, Q.; Luo, F.; Yin, H.; Meng, D. Biogeochemical behavior and pollution control of arsenic in mining areas: A review. Frontier in Microbiology, 2023, 14, 1043024, pp. 1-11. DOI: https://doi.org/10.3389/FMICB.2023.1043024

3. Singh, R.; Singh, S.; Parihar, P.; Singh, V.P.; Prasad, S.M. Arsenic contamination, consequences and remediation techniques: A review. Ecotoxicology and Environmental Safety, 2015, 112, pp. 247–270. DOI: https://doi.org/10.1016/J.ECOENV.2014.10.009

4. Islam, R.; Zhao, L.; Zhang, X.; Liu, L.Z. MiR-218-5p/EGFR signaling in arsenic-induced carcinogenesis. Cancers, 15(4), 1204, pp. 1–15. DOI: https://doi.org/10.3390/cancers15041204

5. Bjorklund, G.; Tippairote, T.; Rahaman, M.S.; Aaseth, J. Developmental toxicity of arsenic: a drift from the classical dose–response relationship. Archives of Toxicology, 2020, 94(1), pp. 67–75. DOI: https://doi.org/10.1007/S00204-019-02628-X

6. Tsuda, T.; Babazono, A.; Ogawa, T.; Hamada, H.; Mino, Y.; Aoyama, H.; Kurumatani, N.; Nagira, T.; Hotta, N.; Harada, M.; Inomata, S. Inorganic arsenic: A dangerous enigma for mankind. Applied Organometallic Chemistry, 1992, 6(4), pp. 309–322. DOI: https://doi.org/10.1002/AOC.590060403

7. Smith, A.H.; Hopenhayn-Rich, C.; Bates, M.N.; Goeden, H.M.; Hertz-Picciotto, I.; Duggan, H.M.; Wood, R.; Kosnett, M.J.; Smith, M.T. Cancer risks from arsenic in drinking water. Environmental Health Perspectives, 1992, 97, pp. 259–267. DOI: https://doi.org/10.1289/EHP.9297259

8. Nordstrom, D.K. Worldwide occurrences of arsenic in ground water. Science, 2002, 296(5576), pp. 2143–2145. DOI: https://doi.org/10.1126/SCIENCE.1072375

9. Oyegoke, T.; Adnan, A. Impact of selected adsorbent functional groups on chromium sorption capacities in an effluent treatment: A DFT study. The Journal of Engineering Research, 2024, 21(1), pp. 59–70. DOI: https://doi.org/10.53540/TJER.VOL21ISS1PP59-70

10. Atieh, M.A.; Bakather, O.Y.; Tawabini, B.S.; Bukhari, A.A.; Khaled, M.; Alharthi, M.; Fettouhi, M.; Abuilaiwi, F.A. Removal of chromium (III) from water by using modified and nonmodified carbon nanotubes. Journal of Nanomaterials, 2010, 1, 232378, pp. 1–9.

DOI: https://doi.org/10.1155/2010/232378

11. Kumar, U.; Bandyopadhyay, M. Sorption of cadmium from aqueous solution using pretreated rice husk. Bioresource Technology, 97(1), pp. 104–109. DOI: https://doi.org/10.1016/J.BIORTECH.2005.02.027

12. Ayedogbon, A.S.; Awoyemi, R.F.; Alabi, A.H. Biosorption of cadmium (II), copper (II) and lead (II) ions by citric acid modified and unmodified cocoa pod shell: Equilibrium, kinetics and thermodynamics. Journal of Science Research, 2015, 14(1), pp. 36–49. https://journals.ui.edu.ng/index.php/jsr/article/view/548

13. Oyegoke, T.; Igwebuike, C.M.; Oyegoke, A. Unraveling the influence of biomaterial's functional groups in Cd biosorption: a density functional theory calculation. Pure and Applied Chemistry, 2024, 96(3), pp. 399–412. DOI: https://doi.org/10.1515/PAC-2023-1103

14. Kumar, M.; Singh, A.K.; Sikandar, M. Study of sorption and desorption of Cd (II) from aqueous solution using isolated green algae Chlorella vulgaris. Applied Water Science, 2018, 8, 225, pp. 1–11. DOI: https://doi.org/10.1007/S13201-018-0871-Y

15. Oyegoke, T.; Oyegoke, A.; Olusanya, J.J. Preliminary investigation on the screening of selected metallic oxides, M_2O_3 (M= Fe, La, and Gd) for the capture of carbon monoxide using a computational approach. The Journal of Engineering, Science and Computing, 2021, 3(1), pp. 1–14. https://jesc.iu.edu.sa/Main/DownloadIssue?IssueId=63&DocFileId=2692

16. Oyegoke, A.; Oyegoke, T.; Olusanya, J.J. Computational study of CO adsorption potential of MgO, SiO_2, Al_2O_3, and Y_2O_3 using a semiempirical quantum calculation method. Nigerian Journal of Materials Science and Engineering, 2021, 11(2), pp. 52–57. https://njmse.msn.ng/Volume11-Issue2-2021/NJMSE-Vol11-Issue2-December-2021_03.pdf

17. Beheshtian, J.; Kamfiroozi, M.; Bagheri, Z.; Ahmadi, A. Computational study of CO and NO adsorption on magnesium oxide nanotubes. Physica E: Low-dimensional Systems and Nanostructures, 2011, 44(3), pp. 546–549. DOI: https://doi.org/10.1016/j.physe.2011.09.016

18. Nagy, T.; Koczka, K.; Haáz, E.; Tóth, A.J.; Rácz, L.; Mizsey, P. Efficiency improvement of CO_2 capture. Periodica Polytechnica Chemical Engineering, 2017, 61(1), pp. 51–58. DOI: https://doi.org/10.3311/PPch.9881

19. Szczęśniak, B.; Choma, J.; Jaroniec, M. Gas adsorption properties of graphene-based materials. Advance Colloidal Interface Science, 2017, 243, pp. 46–59. DOI: https://doi.org/10.1016/J.CIS.2017.03.007

20. Zhou, S.; Liu, J.; Pang, S.; Gui, Y. Adsorption characteristics of H_2S and SO_2 gases on Cu_2O cluster-modified graphene monolayer for gas-sensing applications. ACS Omega, 2023, 8(48), pp. 45763–45773. DOI: https://doi.org/10.1021/ACSOMEGA.3C06310

21. Goswami, A.; Raul, P.K.; Purkait, M.K. Arsenic adsorption using copper (II) oxide nanoparticles. Chemical Engineering Research and Design, 2012, 90(9), pp. 1387–1396. DOI: https://doi.org/10.1016/J.CHERD.2011.12.006

22. Altundogan, H.S.; Altundogan, S.; Tümen, F.; Bildik, M. Arsenic adsorption from aqueous solutions by activated red mud. Waste Management, 2002, 22(3), pp. 357–363. DOI: https://doi.org/10.1016/S0956-053X(01)00041-1

23. Chutia, P.; Kato, S.; Kojima, T.; Satokawa, S. Arsenic adsorption from aqueous solution on synthetic zeolites. Journal of Hazardous Materials, 2009, 162(1), pp. 440–447. DOI: https://doi.org/10.1016/J.JHAZMAT.2008.05.061

24. Tian, Y.; Wu, M.; Lin, X.; Huang, P.; Huang, Y. Synthesis of magnetic wheat straw for arsenic adsorption. Journal of Hazardous Materials, 2011, 193, pp. 10–16. DOI: https://doi.org/10.1016/J.JHAZMAT.2011.04.093

25. Zhang, Y.; Liu, J. Density functional theory study of arsenic adsorption on the Fe_2O_3 (001) surface. Energy & Fuels, 2019, 33(2), pp. 1414–1421. DOI: https://doi.org/10.1021/ACS.ENERGYFUELS.8B04155

26. Watts, H.D.; Tribe, L.; Kubicki, J.D. Arsenic adsorption onto minerals: connecting experimental observations with density functional theory calculations. Minerals, 2014, 4(2), pp. 208–240. DOI: https://doi.org/10.3390/MIN4020208

27. Corum, K.W.; Tamijani, A.A.; Mason, S.E. Density functional theory study of arsenate adsorption onto alumina surfaces. Minerals, 2018, 8(3), 91, pp. 1–18. DOI: https://doi.org/10.3390/MIN8030091

28. Cortés-Arriagada, D.; Ortega, D.E. Removal of arsenic from water using iron-doped phosphorene nanoadsorbents: A theoretical DFT study with solvent effects. Journal of Molecular Liquids, 2020, 307, 112958, pp. 1–8. DOI: https://doi.org/10.1016/J.MOLLIQ.2020.112958

29. Wu, D.; Liu, J.; Yang, Y.; Zhao, Y.; Zheng, Y. The role of SO_2 in arsenic removal by carbon-based sorbents: A DFT study. Chemical Engineering Journal, 2021, 410, 128439, pp. 1–9. DOI: https://doi.org/10.1016/J.CEJ.2021.128439

30. Li, Y.; Sun, X.; Zhou, L.; Ning, P.; Tang, L. Density functional theory analysis of selective adsorption of AsH_3 on transition metal-doped graphene. Journal of Molecular Modeling, 2019, 25(5), 145, pp. 1–12. DOI: https://doi.org/10.1007/S00894-019-3991-X

31. Hehre, W.J. A guide to molecular mechanics and quantum chemical calculations. Wavefunction, 2003, 796 p.

32. Qian, Y.; Yang, H. Computational insight into the bioapplication of 2D materials: A review. Nano Today, 2023, 53, pp. 102007. DOI: https://doi.org/10.1016/J.NANTOD.2023.102007

33. Ayeni, O.I.; Oyegoke, T. Computational insights into graphene-based materials for arsenic removal from wastewater: a hybrid quantum mechanical study. Discover Water, 2024, 4(1), 103, pp. 1–12. DOI: https://doi.org/10.1007/S43832-024-00160-3

34. Oyegoke, T.; Aliyu, A.; Uzochuwu, M.I.; Hassan, Y. Enhancing hydrogen sulphide removal efficiency: A DFT study on selected functionalized graphene-based materials. Carbon Trends, 2024, 15, pp. 100362. DOI: https://doi.org/10.1016/J.CARTRE.2024.100362

35. Tunalı, Ö.F.; Yuksel, N.; Gece, G.; Fellah, M.F. A DFT study of H_2S adsorption and sensing on Ti, V, Cr and Sc doped graphene surfaces. Structural Chemistry, 2024, 35, pp. 759–775. DOI: https://doi.org/10.1007/S11224-023-02265-2

36. Sacanamboy, D.S.; Quispe-Corimayhua, L.; Tilvez, E.A.; Yañez, O. Adsorption of aminomethylphosphonic acid on pristine graphene and graphene doped with transition metals: A theoretical study. Chemical Physics Letters, 2024, 850, pp. 141481. DOI: https://doi.org/10.1016/J.CPLETT.2024.141481

37. Oyegoke, T.; Dabai, F.; Uzairu, A.; Jibril, B. Quantum mechanics calculation of molybdenum and tungsten influence on the CrM-oxide catalyst acidity. Hittite Journal of Science and Engineering, 2020, 7(4), pp. 297–311. DOI: https://doi.org/10.17350/HJSE19030000199

38. Bendjeddou, A.; Abbaz, T.; Gouasmia, A.K.; Villemin, D. Molecular structure, HOMO-LUMO, MEP and Fukui function analysis of some TTF-donor substituted molecules using DFT (B3LYP) calculations. International Research Journal of Pure and Applied Chemistry, 2016, 12(1), pp. 1–9. DOI: https://doi.org/10.9734/irjpac/2016/27066

39. Efil, K.; Bekdemir, Y. Theoretical and experimental investigations on molecular structure, IR, NMR spectra and HOMO-LUMO analysis of 4-methoxy-N-(3-phenylallylidene) aniline. American Journal of Physical Chemistry, 2014, 3(2), pp. 19–25. DOI: https://doi.org/10.11648/j.ajpc.20140302.13

40. Srivastava, M.; Srivastava, A. Cu decorated functionalized graphene for arsenic sensing in water: A first principles analysis. Applied Surface Science, 2021, 560, pp. 149700. DOI: https://doi.org/10.1016/J.APSUSC.2021.149700

41. Supong, A.; Sinha, U.B.; Sinha, D. Density functional theory calculations of the effect of oxygenated functionals on activated carbon towards cresol adsorption. Surfaces, 2022, 5(2), pp. 280–289. DOI: https://doi.org/10.3390/SURFACES5020020

42. Pauling, L. The dependence of bond energy on bond length. Journal of Physical Chemistry, 1954, 58(8), pp. 662–666. DOI: https://doi.org/10.1021/J150518A015

43. Ma, K.; Zheng, D.; Yang, W.; Wu, C.; Dong, S.; Gao, Z.; Zhao, X. A computational study on the adsorption of arsenic pollutants on graphene-based single-atom iron adsorbents. Physical Chemistry Chemical Physics, 2022, 24(21), pp. 13156–13170. DOI: https://doi.org/10.1039/D1CP02170B

44. Lei, M.; Zhang, Y.; Wang, M.; Yang, W.; Gao, Z. Density functional theory investigation of As_4, As_2 and AsH_3 adsorption on Ti-doped graphene. Chemical Engineering Journal, 2021, 421(1), pp. 129747. DOI: https://doi.org/10.1016/J.CEJ.2021.129747